Structural Distortions Induced by Integration Host Factor (IHF) at the H′ Site of Phage λ Probed by (+)-CC-1065, Pluramycin, and $KMnO_4$ and by DNA Cyclization Studies†

Daekyu Sun,‡ Laurence H. Hurley,‡ and Rasika M. Harshey*,§

Department of Microbiology and College of Pharmacy, The University of Texas at Austin, Austin, Texas 78712

Received November 27, 1995; Revised Manuscript Received May 9, 1996⊗

ABSTRACT: Integration Host Factor (IHF) is a sequence-specific DNA-bending protein that is proposed to interact with DNA primarily through the minor groove. We have used various chemical probes [(+)-CC-1065, a minor-groove-specific agent that alkylates N3 of adenine and traps bends into the minor groove; pluramycin, a minor−major-groove threading intercalator that alkylates N7 of guanine; $KMnO_4$, which reacts more strongly with bases in denatured DNA] to gain more information on the interaction of IHF with the H′ site of phage λ. In addition to the 13-bp core consensus recognition element present at all IHF binding sites, the H′ site also has an upstream AT-rich element that increases the affinity of IHF for this site. Our results reveal new details of IHF−DNA interaction at this site. Results with (+)-CC-1065 modification suggest that IHF interacts with the adenines on the 3′-side of the AT-rich element and likely induces a minor-groove bend in its vicinity, which in turn stabilizes the interaction. Pluramycin modification experiments suggest the presence of both short- and long-range structural perturbations (possible DNA unwinding events) on either side of the IHF contact region. Although IHF is known to induce a large bend in DNA at the H′ site, no separation of base pairs was detected when the bent DNA was probed with $KMnO_4$. DNA cyclization studies indicate a large magnitude (approximately 180°) for the IHF-induced bend at the H′ site, consistent with >140° bend estimated by gel electrophoresis methods. These studies suggest that IHF-induced DNA bending is accompanied by the introduction of a DNA node, DNA unwinding, and/or by some other DNA distortion. An enhanced binding and stability of IHF was observed on small circular DNA.

Integration Host Factor (IHF) is a small (20 000 M_r), heterodimeric, sequence-specific DNA-binding protein of *Escherichia coli* that regulates a large number of DNA−protein transactions, including site-specific recombination, replication, packaging, and gene expression [reviewed in Friedman (1988), Freundlich et al. (1992), and Goosen and van de Putte (1995)]. Through comparison of several IHF binding sites, a degenerate core consensus sequence, WATCAANNNNTTR (where W is A or T, R is A or G, and N is any nucleotide; Friedman, 1988), has been defined that includes an AT-rich element on the 5′-side (Goodrich et al., 1990). Although the upstream element is not found at all sites, it is required for IHF binding at some sites and enhances binding significantly at others (Hales et al., 1994). Photo-cross-linking of IHF to DNA has revealed close protein−DNA contacts at this upstream site (Yang & Nash, 1994).

Footprinting studies with alkylating agents and hydroxyl radicals using λ *att* sites have suggested that IHF recognizes DNA primarily through contacts within the minor groove (Yang & Nash, 1989). Similar conclusions were reached in studies with other IHF binding sites (Winkelman & Hatfield, 1990; Panigrahi & Walker, 1991). More recent studies using base analogs have suggested that IHF interactions with the consensus sequence at the H′ site also occur within the major groove (Wang et al., 1995). No structural information on the protein is yet available, but on the basis of the structure of a related protein HU from *Bacillus stearothermophilus* (Tanaka et al., 1984), models for IHF−DNA interaction have been proposed (Yang & Nash, 1989; White et al., 1989).

The unusual, largely minor-groove IHF−DNA interaction inferred from footprinting studies prompted us to use the minor-groove-specific drug (+)-CC-1065 (see Figure 1A) as a structural probe to study this interaction. We have recently used this drug to dissect interactions of the Mu transposase (Ding et al., 1993), transcription factor Sp1 (Sun & Hurley, 1994a,b), and TFIID (Sun & Hurley, 1995) with their cognate sites. In the case of Mu transposase, (+)-CC-1065 proved to be a useful probe to distinguish protein protection sites from minor-groove narrowing sites (Ding et al., 1993). (+)-CC-1065 is a potent antitumor antibiotic that binds duplex DNA, overlapping in the minor groove a 4- and 1-bp region on the 5′- and 3′-sides, respectively, of the modified adenine (Hurley et al., 1984; Reynolds et al., 1985; Scahill et al., 1990). Only adenines in certain sequences, such as 5′PuNTTA* and 5′AAAAA* (* indicates the covalently modified adenine), are reactive toward (+)-CC-1065 at the lowest drug concentrations (Reynolds et al., 1985). As a consequence of formation of a (+)-CC-1065−(N3-adenine)-DNA adduct, (+)-CC-1065 induces bending, winding, and stiffening of DNA (Lee et al., 1991; Sun & Hurley, 1992; Sun et al., 1993a). DNA flexibility, in particular, the propensity to form a bent DNA structure as a

† This research was supported by grants from the Public Health Service (CA-49751), the Welch Foundation, and the Burroughs Wellcome Scholars Program to L.H. and by the National Institutes of Health (GM 33247) to R.H.

* To whom correspondence should be addressed.

‡ College of Pharmacy.

§ Department of Microbiology.

⊗ Abstract published in *Advance ACS Abstracts,* August 1, 1996.

S0006-2960(95)02786-3 CCC: $12.00

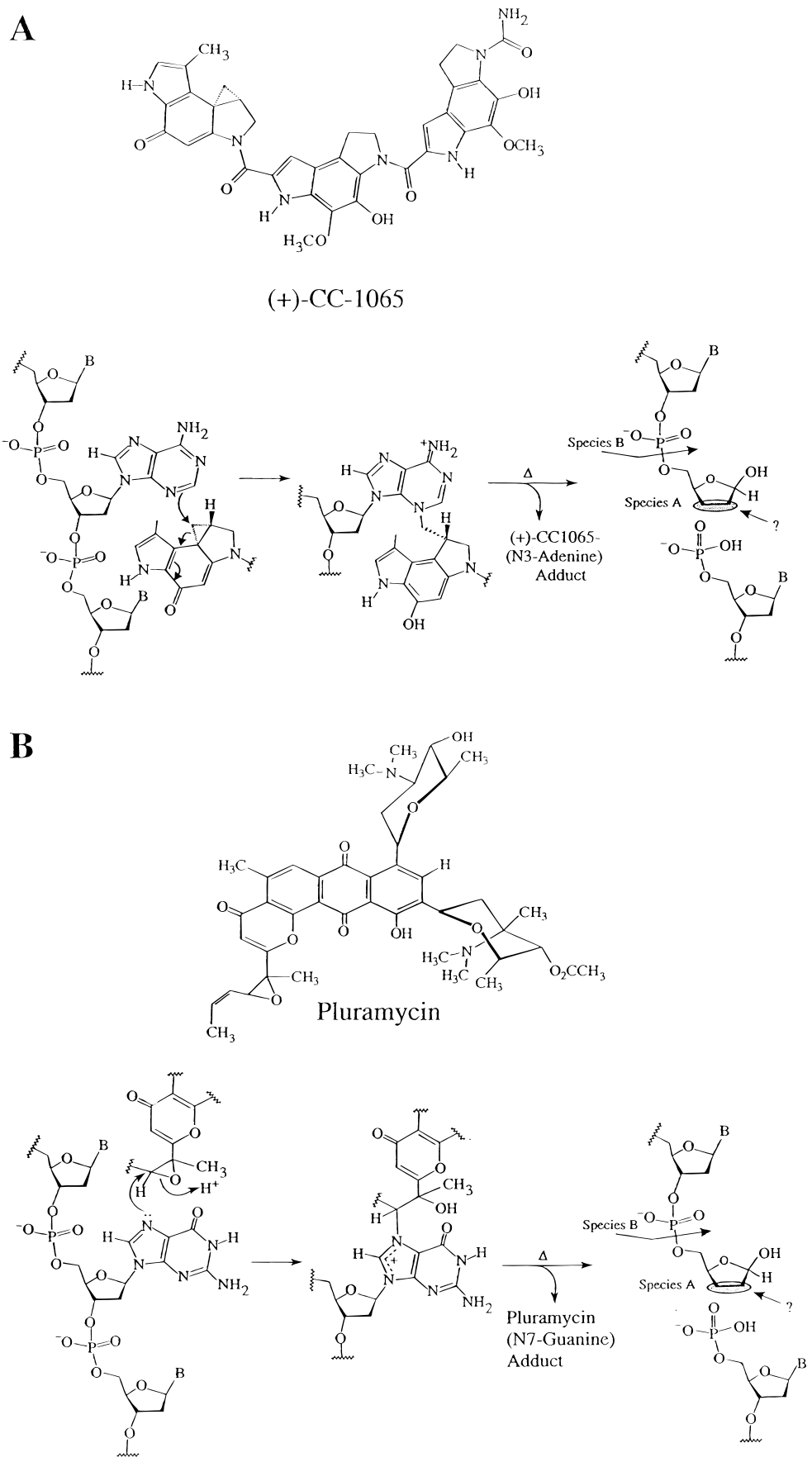

FIGURE 1: (A) Structure of (+)-CC-1065, reaction with DNA to form the (+)-CC-1065−(N3-adenine)-DNA adduct, and thermally induced strand breakage of the (+)-CC-1065−DNA adduct. Species A is the product produced by thermal treatment and species B is the product produced by thermal and subsequent piperidine treatment. (B) Structure of pluramycin, reaction of pluramycin with DNA to form the pluramycin−(N7-adenine)-DNA adduct, and products of thermal and piperidine cleavage of the DNA adduct.

Table 1: DNA Sequences of Oligomer Duplexes Used in This Study

I	5′ GTCGCGTAAGTTGGCATTATAAAAAAGCATTGCTTATCAATTTGTTGCAACGAACAGGTCACTGAATGCGCTGA 3′ 3′ CAGCGCATTCAACCGTAATATTTTTTCGTAACGAATAGTTAAACAACGTTGCTTGTCCAGTGACTTACGCGACT 5′
II	5′ CGCTGCGCGCGATCGGGCATTATAAAAAAGCATTGCTTATCAATTTGTTGCAACGAACAGGTCACGCAACGCGGTGA 3′ 3′ ACGCGCGCTAGCCCGTAATATTTTTTCGTAACGAATAGTTAAACAACGTTGCTTGTCCAGTGCGTTGCGCCACTGCG 5′

consequence of covalent bonding, has been identified as an important component of sequence recognition of this drug (Hurley et al., 1988; Warpehoski & Hurley, 1988). (+)-CC-1065 is therefore also a DNA bending probe (Sun et al., 1993a).

We have used two other reagents, pluramycin and $KMnO_4$, in this study to probe structural distortions associated with IHFs. Pluramycin (Figure 1B) belongs to the family of antitumor antibiotics called "threading" intercalators, since they project into both the major and minor grooves at the site of intercalation, forming covalent adducts with N7 of guanine at the 3′-side of the intercalation site, accompanied by DNA unwinding (Sun et al., 1993b, 1995; Hansen et al., 1995). Unwinding of DNA is therefore expected to facilitate pluramycin intercalation at that site. $KMnO_4$ oxidizes unpaired bases in DNA (Hayatsu & Ukita, 1967; Sasse-Dwight & Gralla, 1988). Although $KMnO_4$ is reported to be pyrimidine-specific, preferentially oxidizing thymine in single-stranded DNA, it has also been reported to modify purines in denatured DNA (Akman et al., 1990). Thus, $KMnO_4$ should report on the presence of single-stranded regions accompanying the DNA distortions induced by IHF binding.

The ability of IHF to bend DNA (Robertson & Nash, 1988) is thought to be important for its varied functions (Goodman et al., 1992). Large IHF-induced bends (>140°) have been inferred at three IHF binding sites found within the *att* sites of phage λ (H′, H1, and H2) using polyacrylamide gel electrophoresis (Thompson & Landy, 1988), and at λ cos sites using electron microscopy (Kosturko et al., 1989). In this report we have estimated the extent of IHF-induced DNA bending at the H′ site using the method of DNA cyclization. In the past, such studies have yielded an excellent agreement between the estimated bending magnitude and that determined by X-ray studies (Lyubchenko et al., 1991).

Our results using these specific DNA conformational probes and circularization experiments provide new insights into the structure of the IHF−H′-site DNA complex that show distortion both within and outside the DNA binding region.

EXPERIMENTAL PROCEDURES

Materials. IHF was kindly provided by Howard A. Nash (NIH), (+)-CC-1065 by Patrick McGovren (The Upjohn Co.), and pluramycin by Abbott Laboratories (Chicago, IL). T4 DNA ligase was from New England Biolabs, and T4 polynucleotide kinase was from U.S. Biochemical Co. [γ-^{32}P]ATP[1] was purchased from ICN. Electrophoretic reagents [acrylamide/bis(acrylamide), *N*,*N*,*N*′,*N*′-tetramethylethylenediamine, and ammonium persulfate] were purchased from Bio-Rad, and X-ray film, intensifying screens, and developing chemicals were from Amersham. The 74- and 77-bp oligomer duplexes (I and II) containing the H′ site of phage λ (Table 1) were synthesized on an automated DNA synthesizer (Applied Biosystems 381A) using the phosphoramidate method. Oligonucleotides were deprotected in concentrated ammonium hydroxide at 55 °C overnight, dried under vacuum, and purified on 8% denaturing acrylamide gels. They were then 5′-end-labeled with ^{32}P and annealed, as described previously (Lee et al., 1991).

Formation of IHF−DNA Complexes and Mobility Shift Assays. IHF−DNA complexes were formed in a 25-μL solution containing 5 ng of 5′-end-labeled DNA, 50 mM Tris-HCl (pH 7.6), 10 mM $MgCl_2$, 0.1 mM EDTA, 5% glycerol, 40 mM KCl, and indicated amounts of protein. When products of DNA cyclization were complexed with IHF, 0.5 ng of end-labeled DNA was used. The samples were incubated at 30 °C for 15 min and loaded onto a 5% native polyacrylamide gel (acrylamide:bisacrylamide 29:1) in Tris−borate−EDTA buffer (50 mM Tris/50 mM boric acid/1 mM EDTA, pH 8.3) to separate protein−DNA complexes from free DNA. Electrophoresis was carried out at room temperature at 280 V for 3 h.

DNase I Footprinting. IHF−DNA complexes were formed and digested with DNase I (0.2 unit) for 1 min. Reactions were stopped by the addition of 2 volumes of alkaline dye (80% formamide, 10 mM NaOH).

Hydroxyl-Radical Footprinting. IHF−DNA complexes were formed as described above in a molar ratio of 1:1 (DNA:protein). After 15 min at 30 °C, 2 μL of freshly made stocks of 2 mM iron−EDTA, 2% hydrogen peroxide, and 10 mM sodium ascorbate were added. After 2 min the reactions were stopped by the addition of glycerol (5%) and electrophoresed in polyacrylamide gels to separate protein by soaking appropriate pieces of the gel in buffer overnight. After ethanol precipitation, DNA pellets were dried and redissolved in alkaline dye.

$KMnO_4$ and DMS Protection. Preformed IHF−DNA complexes were reacted with 0.1 volume of 5% DMS in ethanol or 2 mM (final concentration) $KMnO_4$. After 2 min the samples were electrophoresed as above to separate and isolate protein−DNA complexes from free DNA. DNA pellets were dissolved in 20 μL of 1 M piperidine and heated at 95 °C for 15 min to induce strand breakage. Samples were dried under vacuum and redissolved in alkaline dye solution.

(+)-CC-1065 and Pluramycin Protection Experiments. For time course experiments, IHF−DNA complexes or free DNA were treated at 30 °C with 0.5 μM or 0.1 μM (final) amounts of either (+)-CC-1065 or pluramycin, respectively. At various times, the reactions were stopped by withdrawing 10-μL aliquots and mixing with 100 μL of distilled water containing 10 μg of calf thymus DNA. Unreacted drug

[1] Abbreviations: bp, base pair; EDTA, ethylenediaminetetraacetic acid; Tris, tris(hydroxymethyl)aminomethane; A-tract, adenine tract; SDS, sodium dodecyl sulfate; ATP, adenosine triphosphate; DMS, dimethylsulfate.

molecules were removed by phenol/chloroform extraction followed by ethanol precipitation. The DNA samples were finally dissolved in distilled water and subjected to thermal treatment (boiling for 30 min) to induce DNA strand breakage at the drug modification sites. In other experiments, preformed IHF−DNA complexes were treated with (+)-CC-1065 or pluramycin for 2 min at 30 °C and loaded onto native polyacrylamide gels to separate protein−DNA complexes from free DNA, as described above in the $KMnO_4$ and DMS protection experiments. In some experiments, DNA samples were heated up to 95 °C for 15 min in the presence of 1 M piperidine to induce DNA strand breakage at the pluramycin modification sites.

Cyclization Experiments and Product Analysis. Oligomer II (Table 1) was designed to expose a three-nucleotide asymmetric overhang so as to ensure head-to-tail ligation. The H′ site is approximately at the center of the sequence. About 2 ng of ^{32}P-labeled oligomer II was incubated for 15 min at 30 °C with a 2-fold molar excess of IHF (2 ng) in 20 μL of T4 ligase buffer [25 mM Tris-HCl (pH 7.6), 5 mM $MgCl_2$, 25 μg/mL bovine serum albumin, 1 mM ATP, and 5 mM dithiothreitol]. Reactions were initiated by the addition of 100 units of T4 DNA ligase and terminated after incubation for 30 min by the addition of SDS to 0.5% followed by phenol/chloroform extraction and ethanol precipitation. Ligation products were separated on a 6% polyacrylamide gel. For time course experiments, 20 ng of DNA was incubated with 20 ng of IHF in 100 μL of reaction buffer, and 1000 units of T4 DNA ligase was added to initiate ligation. Reactions were terminated at various times by the addition of SDS (final 0.5%). For size determination, each band was excised from the gel, purified, and analyzed on a 4% denaturing polyacrylamide gel, as described previously (Ulanovsky et al., 1986).

RESULTS

Hydroxyl-Radical Footprinting. The DNA substrates for all experiments described in this study were designed to contain the sequences corresponding to the H′ IHF recognition site of phage λ. (See Table 1; oligomer I was used primarily in chemical modification experiments, while II was used in cyclization studies. Both oligomers have identical 55-bp sequences overlapping the IHF binding site.) Earlier hydroxyl-radical footprinting and alkylation protection/interference experiments have suggested that IHF recognizes determinants in the minor groove (Yang & Nash, 1989). To ascertain whether the reported IHF−DNA interaction could be reproduced under our experimental conditions, we treated IHF−DNA complexes with hydroxyl radicals and separated protein-bound DNA (B) from protein-free DNA (F) by native gel electrophoresis. DNA from the B and F species, as well as from a control sample (I) not bound to IHF, was isolated and electrophoresed on denaturing polyacrylamide gels. Figure 2, panels A and B, shows the footprints on the upper (+) and lower (−) strands of each DNA species, respectively. Quantitative analysis of the cleavage patterns reveals that, as demonstrated before (Yang & Nash, 1989), three protected regions are clearly visible, separated by two regions at which hydroxyl-radical cleavage is even greater in the presence of IHF than that seen in its absence. These results are summarized in Figure 2C, along with the results of DMS protection experiments (not shown). The latter experiments reveal that, as described before (Yang & Nash, 1989), the IHF−DNA interaction occurs over approximately 30 bp at the H′ site (which includes the core element as well as the upstream AT-rich element), mainly through the minor groove (17/22 adenines are protected from methylation, as opposed to 3/8 guanines). Two of the three guanines protected are within the consensus, suggestive of some major-groove contacts in this region as well, as recently demonstrated by Wang and co-workers (1995).

In the Presence of IHF, (+)-CC-1065 Interacts with the 3′-Side Adenines of the Upstream A-Tract but Not within the Consensus Sequence. In this study, (+)-CC-1065 was used as a minor-groove probe as well as a DNA bending probe. As shown earlier (Yang & Nash, 1989), and in Figure 2 and elsewhere, IHF shows a very broad region of footprinting when hydroxyl radicals or DNase I (Figure 3) are used as footprinting reagents. These two reagents are sensitive not only to direct contacts between protein and DNA but also to structural changes in DNA. For example, hydroxyl-radical attack is known to be strongly influenced by the width of the minor groove, a narrower minor groove being associated with diminished attack (Burkhoff & Tullius, 1987, 1988). It has been shown, in the case of phage Mu transposase, that two regions in its cognate site exhibiting hydroxyl-radical protection are likely not the result of protein protection but rather regions of narrower minor grooves (Ding et al., 1993). Not only was (+)-CC-1065 modification of DNA at these sites tolerated by the Mu transposase, but these sites were preferred drug modification sites in the presence of the transposase. Thus, (+)-CC-1065 proved a useful tool for discriminating protein protection sites from minor-groove narrowing or bending sites.

To determine whether the IHF-induced modulation of DNase I and hydroxyl-radical cleavage were due to structural changes in DNA structure, such as bending, or due to direct contact by protein, we monitored modification of the H′ site by (+)-CC-1065 in the presence of increasing amounts of IHF. As shown in Figure 3, and consistent with previous reports, the 5′ upstream A-tract region shows DNase I protection as well as hydroxyl-radical protection (see Figure 2) in the presence of IHF. On the top strand, (+)-CC-1065 alkylation sites occur in adenines at the 3′-side of the AT region. However, upon interaction with IHF, the alkylation sites move from the 3′- to the 5′-end of the A-tract (see lanes 6−9 in Figure 3). These results suggest either that IHF makes direct contacts with the 3′-end of the A-tract, which blocks access to the drug, or that structural changes induced at this end by IHF interactions elsewhere are responsible for the shift in (+)-CC-1065 interaction to the 5′-end of the A-tract. Recent cross-linking experiments place IHF in close proximity to the 3′-end of the A-tract (Yang & Nash, 1994), lending credence to the former notion. We note that no other (+)-CC-1065 modification sites are found within the IHF binding region on this strand.

The above results were investigated in more detail by following the time course of (+)-CC-1065 modification on both strands in the absence and presence of IHF (Figure 4A,B). In accord with the results shown in Figure 3, the time course experiment shows a shift of alkylation by (+)-CC-1065 to the 5′-side of the A-tract in the presence of IHF (Figure 4A). On the bottom strand (B), there were three weak or moderate alkylation sites within the core consensus sequence. All alkylation sites were protected from modification in the presence of IHF. These results exclude the

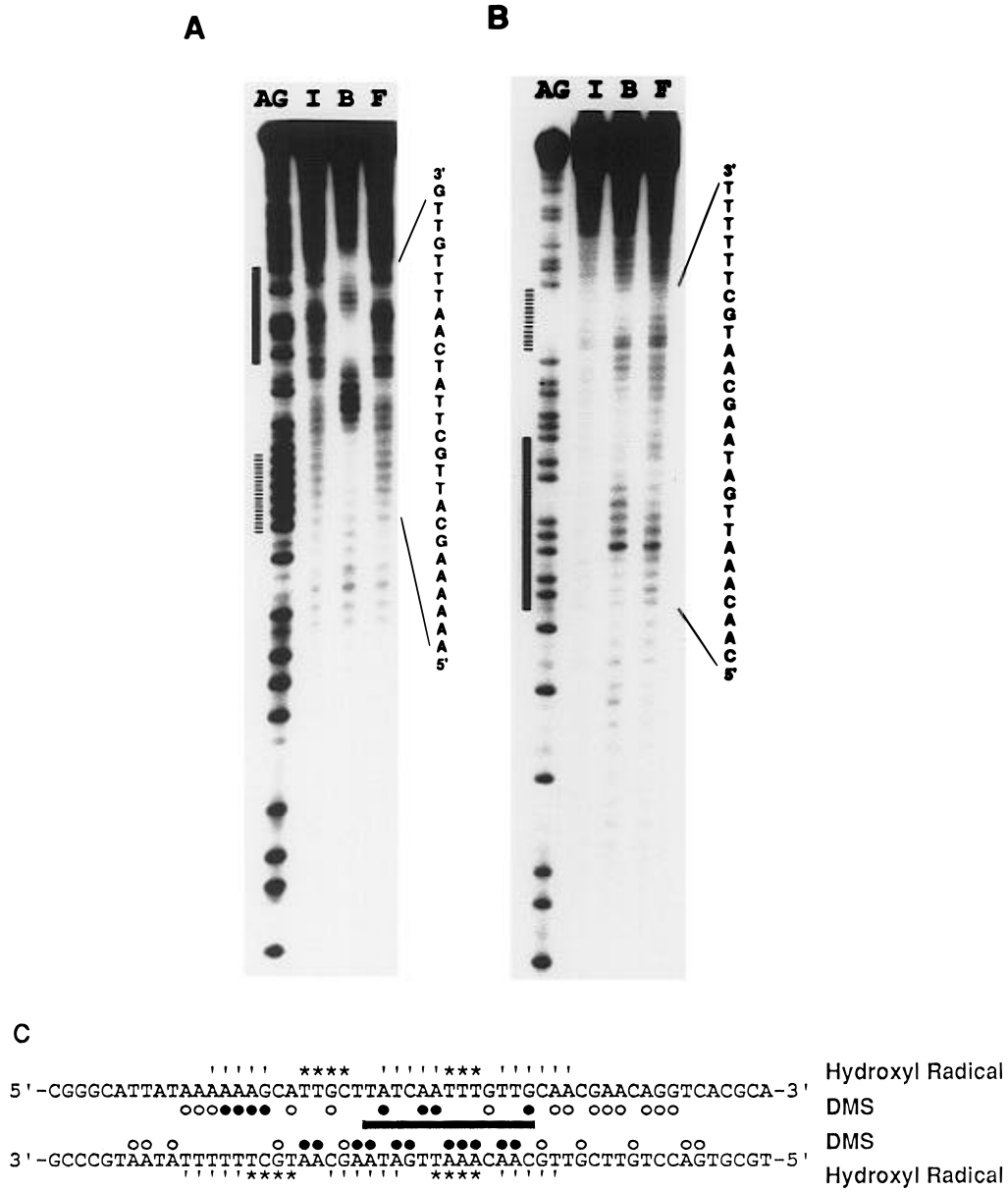

FIGURE 2: Hydroxyl-radical footprints of IHF−DNA complexes. Complexes made with oligomer II (Table 1) were subjected to hydroxyl-radical cleavage, after which bound (B) and free (F) DNA fragments were isolated following separation by electrophoresis on a native polyacrylamide gel. These DNA species were next electrophoresed on denaturing polyacrylamide gels along with DNA subjected to hydroxyl-radical treatment in the absence of IHF (I). (A) and (B) show data obtained for the top and bottom strands, respectively. Purine-specific Maxam−Gilbert cleavage reaction is labeled **AG**. The core consensus sequence is indicated by a solid bar and the AT-rich region by a hatched bar. The sequences are shown to the right side of the panels. (C) Summary of experimentally determined footprints. The core consensus sequence is indicated by a solid bar. For hydroxyl-radical footprints, an asterisk indicates enhanced hydroxyl-radical cleavage and a prime indicates protection from hydroxyl radicals. Filled and open symbols indicate protection and nonprotection, respectively, from DMS.

possibility that the observed hydroxyl-radical protection within this region (see Figure 2) might be the result of a purely structural change, such as narrowing of the minor groove, and are in accord with the deduction that IHF interacts within this region through the minor groove. Consistent with results from the top strand (shown in Figures 3 and 4A), there is an enhanced reaction of (+)-CC-1065 with an adenine on the 3′-side of the AT-rich region on the bottom strand as well (Figure 4B). However, protection of a neighboring 5′-side of adenine at the same region (bottom strand) suggests that IHF makes direct contacts with this region, thereby blocking access to the drug. [Recall that (+)-CC-1065 occupies a stretch of 4 bp on the 5′-side of the alkylated adenine.] These results are summarized in Figure 4C. Since minor-groove bends are favored sites for (+)-CC-1065 modification (Reynolds et al., 1985; Sun et al., 1993a), these observations suggest that IHF interaction with the 3′-end of the A-tract induces a minor-groove bend that is manifested at the 5′-end and recognized by (+)-CC-1065 as a high-reactivity site.

(+)-CC-1065 Modification of 5′ Adenines in the AT-Rich Element Stabilizes IHF Binding. In the following experiments, we monitored the effects of prior (+)-CC-1065 modification of DNA on IHF binding. First, IHF−DNA complexes were treated with (+)-CC-1065 and electrophoresed on a native polyacrylamide gel to separate protein-bound DNA (B) from free DNA (F) (Figure 5A, lanes 2 and 4, top and bottom strand radiolabeled, respectively). Each species of DNA was isolated, along with untreated controls (I) (lanes 1 and 3 in Figure 5A), and thermally cleaved to determine

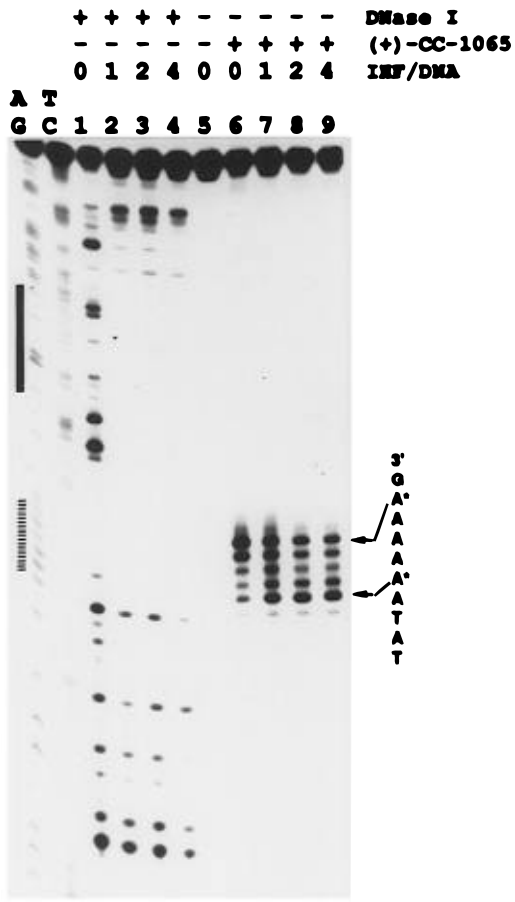

FIGURE 3: Effect of IHF binding on the pattern of (+)-CC-1065 modification of the top strand of H′ DNA. Lanes 1−4, DNase I cleavage pattern of IHF−DNA complexes with increasing amounts of IHF (molar ratios are indicated). Lane 5, control DNA (oligomer I) without (+)-CC-1065 treatment. Lanes 6−9, (+)-CC-1065-modified complexes (reaction time, 5 min at 30 °C). Arrows point to the major adenines modified with (+)-CC-1065 (*) within the AT-rich element. Multiple strand breakage sites are expected, based on the thermal cleavage pattern shown in Figure 1A (species A and B). Other breakages are due to minor alkylation sites. **AG** and **TC** are Maxam−Gilbert sequencing reactions. Other symbols are as in Figure 2.

(+)-CC-1065 modification sites. Figure 5, B and C, shows the pattern of cleavage of the top- and bottom-strand-labeled DNA species, respectively. The alkylation patterns observed for the bound and free forms of DNA were consistent with the patterns seen in solution (Figure 4), in that DNA in protein-bound complexes was specifically enriched in adenines modified within the 5′ region of the AT-rich element, while DNA with adenines modified within the core consensus sequence was excluded from the complexes.

Next, a gel retardation assay (Figure 6) was used to evaluate the relative affinity of IHF for DNA extracted from the three different species: B, F, and I. IHF was complexed with each DNA species, challenged with a 20-fold excess of cold DNA for the indicated period of time, and electrophoresed on native polyacrylamide gels. As seen in Figure 6, (+)-CC-1065-modified DNA isolated from protein−DNA complexes and rebound with IHF (middle panel) shows a slower rate of dissociation of IHF than that from complexes formed with unmodified control DNA (left panel). (+)-CC-1065-modified DNA isolated from the free DNA species (right panel) shows a poor affinity for IHF, compared to both unmodified DNA and DNA isolated from modified protein−DNA complexes. Thus, modification of 5′ adenines in the AT-rich element stabilizes the IHF−DNA interaction.

Pluramycin Shows Enhanced Reactivity Upstream and Downstream of the IHF Consensus Sequence. To identify pluramycin intercalation (and hence possible unwinding) sites generated by IHF binding to the H′ site, we looked for enhanced pluramycin alkylation sites in IHF−DNA complexes. Figure 7 shows the results, with DNA labeled on the top (A) or bottom (B) strands, in the absence (lanes 2−3) and presence (lanes 4−5) of IHF. In the presence of IHF, pluramycin alkylation sites on both strands within the region spanning the AT-rich element and the core consensus sequence are protected, while sites outside this region are either unprotected or enhanced (summarized in Figure 7C).[2] We note that some of the enhanced sites lie outside the 30-bp IHF interaction site, as defined by DMS and hydroxyl-radical footprinting experiments (see Figure 2), but within the DNase I-protected region, while others lie even further outside. These enhanced pluramycin modification sites either represent DNA unwinding sites or some other change in the DNA groove geometry that promotes effective intercalation. The results suggest that the effect of IHF binding can be propagated on DNA over a long range on both sides of its binding site.

In a separate experiment, pluramycin was added to preformed IHF−DNA complexes. IHF-bound DNA was separated from unbound or free DNA and isolated along with control DNA treated with pluramycin in the absence of IHF, as described previously for (+)-CC-1065 modification (see Figure 5). As before, the DNA was subjected to thermal strand breakage to determine the extent and site selectivity of pluramycin modification in the different DNA species on the (+) and (−) strands. In accord with the protection experiments shown in Figure 7, protein-bound complexes are specifically enriched in pluramycin-modified guanine residues flanking the upstream and downstream sides of the IHF consensus sequence, corresponding to the enhancement sites shown in Figure 7C (data not shown).

$KMnO_4$ Protection Experiments. DNA unwinding is sometimes accompanied by base-pair separation, as exemplified by the SV40 viral T antigen−DNA interaction (Borowiec & Hurwitz, 1988). In order to test whether this is also true for IHF, $KMnO_4$ was used as a chemical probe. It is generally accepted that the primary cause of $KMnO_4$ reactivity with thymines in an AT region is unpairing of the DNA duplex (Borowiec & Hurwitz, 1988; Frantz & O'Halloran, 1990). As shown in Figure 8, IHF strongly protects the overall region of the consensus sequence from $KMnO_4$ modification, implying an absence of strand separation in this region. Interestingly, the *thymine* tracts on the upstream region of the IHF core consensus sequence are most strongly protected from $KMnO_4$ attack (see region between arrows to the right of panel B in Figure 8). In light of the observation that $KMnO_4$ has a lower reactivity in DNA regions that are stably bent as well as in those that make direct contacts with protein (McCarthy et al., 1993), the

[2] Each of the lanes was scanned using a densitometer to normalize for the amount of radioactivity at the top of the gel. Visual inspection of the bands at the top of the gel may be misleading, because while the photograph merges the unmodified DNA band with a strong breakage site, the original gel shows a demarcation between the bands. Only those bands that showed reproducible enhancement at both time points were included in Figure 7C.

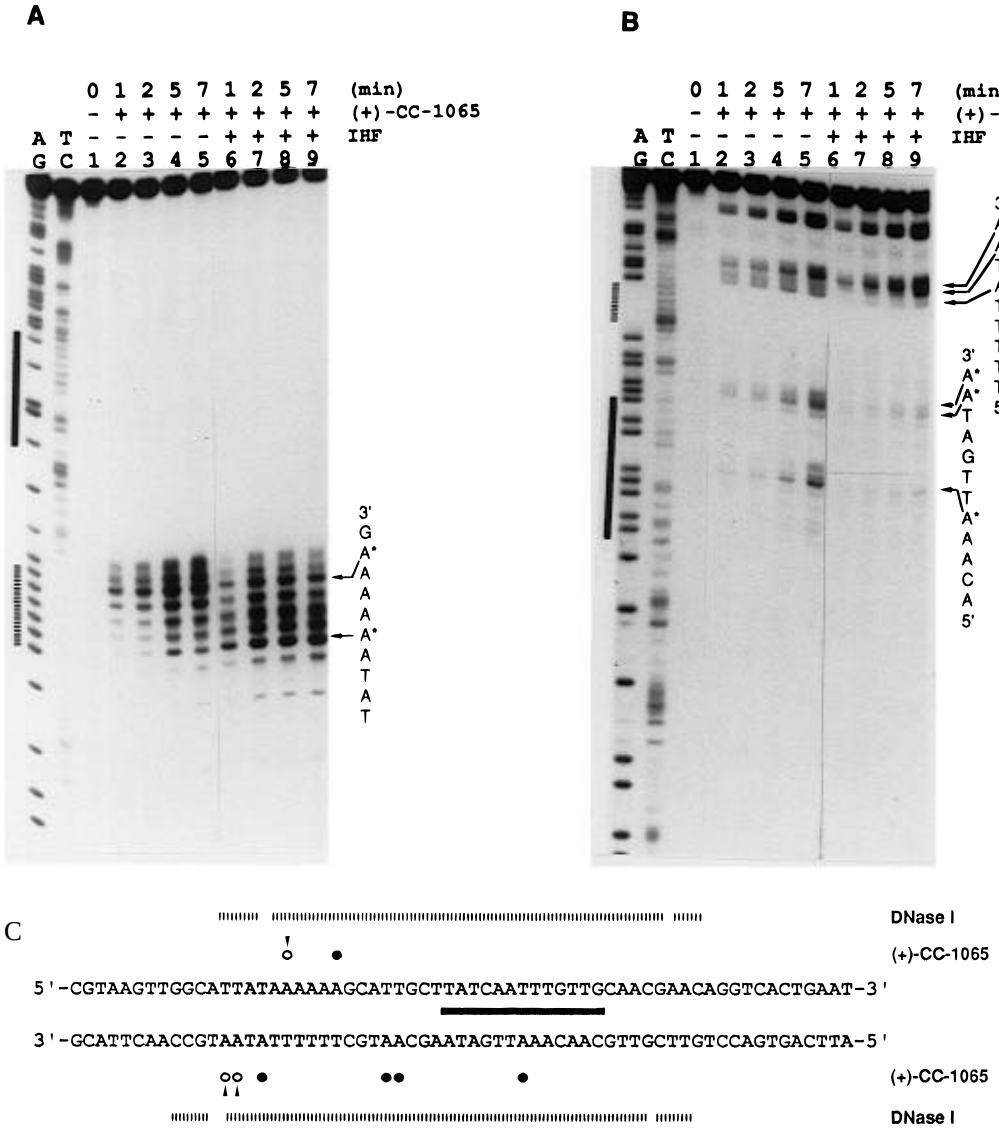

FIGURE 4: Time course of (+)-CC-1065 modification of DNA in the presence of IHF. Modification of protein-free oligomer I DNA (lanes 2−5) and IHF-complexed DNA (lanes 6−9) with (+)-CC-1065 is shown. Lane 1, unmodified control DNA. (A) and (B) show data for the top and bottom strands. To form the IHF−DNA complex, a 2-fold molar excess of IHF was added to the reaction mixtures. Other symbols are as in Figure 3. (C) Summary of (+)-CC-1065 protection experiments. Closed and open circles indicate (+)-CC-1065 protection and modification sites, respectively. Arrowheads indicate enhanced modification sites.

results in Figure 8 support the idea that IHF binding induces a bend in the DNA at the upstream A-tract region.

IHF-Induced DNA Cyclization. Oligomer II (Table 1) was the substrate for DNA cyclization experiments. The results of ligating this DNA in the absence and presence of IHF are shown in Figure 9. In the absence of IHF, T4 DNA ligase converted the 77-bp DNA (M) into products that migrated at the position of linear multimers [mainly dimers (D) and trimers (T)] as well as a small amount of circular dimer (II) and trimer species (III). Ligation in the presence of IHF reduced the linear multimers and circular trimer species and resulted (within 2 min) in the production of a circular dimer (II; see below) as well as a new species, designated I. The complete absence of a circular trimer species in the presence of IHF argues strongly that the induced bend has magnitude closer to 180° than to 120°.

Characterization of Ligation Products. The identity of each ligation product shown in Figure 9 was determined by elution of individual bands from the native gel and analysis in a denaturing polyacrylamide gel (Figure 10). The 77-bp linear DNA fragment and higher molecular weight linear species formed in the presence of T4 DNA ligase (lanes 1−5) migrated at expected sizes for linear monomer, dimer, trimer, tetramer, and pentamer species. The presence of lower molecular weight species in each of these lanes is likely the result of incomplete ligation of one of the strands in the duplex oligomer. Bands labeled I and II in Figure 9B each gave rise to three similar bands (a−c) on the denaturing gel (lanes 6 and 7). Band a corresponds to the size of a single-stranded linear dimer (154 bp). Bands b and c migrate at positions appropriate for single- and double-stranded circular forms of the dimer (Ulanovsky et al., 1986). We interpret these data to suggest that both I and II are different forms of a circular dimeric species. Species I (lane 6; note the roughly equal amounts of bands a and b in this lane) has more of band c (putative double-stranded circular form) than species II, suggesting that species II is likely a nicked form of the covalently closed species I.

In order to further characterize the ligation products obtained in the presence of IHF, two-dimensional gel

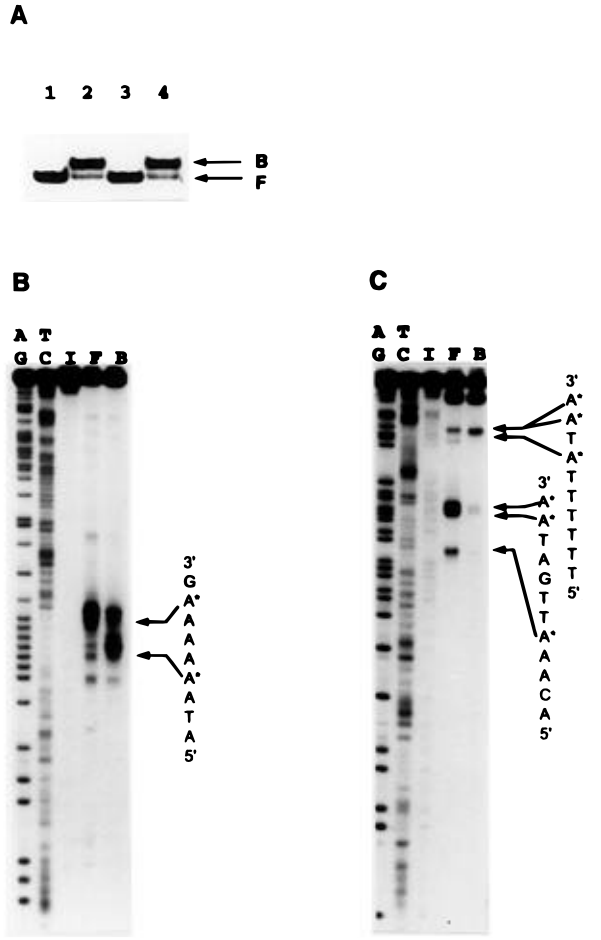

FIGURE 5: Effect of (+)-CC-1065 modification on the formation of IHF−DNA complexes. (A) Complexes were formed with DNA substrates labeled on the top (lane 2) or bottom strands (lane 4), treated with (+)-CC-1065 for 5 min, and electrophoresed on a native polyacrylamide gel. Lanes 1 and 3 contain appropriately labeled unmodified control DNA. The bound (B), free (F), and control (I) DNA fragments thus separated were isolated, thermally cleaved, and electrophoresed on denaturing polyacrylamide gels to monitor (+)-CC-1065 modification sites. (B) and (C) show data for the top and bottom strands, respectively. Symbols are as in Figure 3.

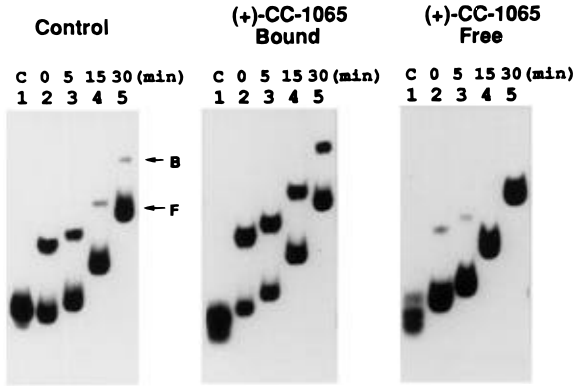

FIGURE 6: Measurement of the relative rates of dissociation of IHF complexed with (+)-CC-1065-unmodified control DNA (left), modified DNA recovered from IHF-bound complexes (middle), and modified DNA recovered from unbound or free complexes (right) obtained from the experiment shown in Figure 5. IHF complexes formed with each of the three species of DNA were challenged with a 20-fold excess of cold DNA for the indicated times and then applied to native polyacrylamide gels for electrophoresis. The bound (B) and unbound (F) forms of the DNA are indicated.

electrophoresis was carried out, adding chloroquine phosphate, a DNA intercalator, to the running buffer during electrophoresis in the second dimension (data not shown). By unwinding closed circular DNA, chloroquine phosphate reduces DNA twist and results in an increase in DNA writhe. If the DNA is initially relaxed, increasing the concentration of the intercalator will cause an incremental increase in both positive writhe and gel mobility until the DNA eventually migrates as an unresolved band. Alternatively, if DNA is initially negatively or positively supercoiled, and hence has negative or positive writhe, intercalation of chloroquine will eventually lower the mobility of negatively supercoiled DNA to that of relaxed DNA, whereas it will increase the mobility of positively supercoiled DNA. Chloroquine phosphate should not change the mobility of linear or nicked circular DNA since the reduction in twist in these DNAs manifests itself merely as a swiveling of one strand around the other, and no writhing takes place. The linear multimers, as well as species II, maintained their migration positions in both dimensions, suggesting that species II is a nicked form of circular DNA. DNA corresponding to species I, however, migrated more slowly in the second dimension, suggesting that species I is likely negatively supercoiled and/or carries some other DNA distortion that increases its mobility in native polyacrylamide gels (Figure 9), the latter state being correctable by chloroquine. In support of these assignments species II was resistant to the action of calf thymus topoisomerase I, while treatment of species I with this enzyme converted it into species II, albeit poorly (data not shown). Species I was also a poor substrate for rebinding IHF (see below).

IHF Shows an Enhanced Affinity for Circular DNA. Most protein−DNA interactions are accompanied by significant changes in DNA conformation. Conversely, preinduced conformational changes in DNA can be expected to enhance the binding affinity of their cognate proteins (see Pil et al., 1993). In order to test if the circular ligation products generated in the presence of IHF had generated a DNA conformation favorable to binding IHF, we compared IHF binding to linear and circular dimers (Figure 11A). With increasing concentrations of IHF, two slower migrating complexes (CI and CII) were seen with linear dimeric DNA (left panel), consistent with occupation by IHF of one or two sites in the dimer. IHF had a higher affinity for the circular dimer II compared to linear dimer DNA (compare left and middle panels), resulting in two faster migrating complexes, which is consistent with the generation of sharp bends that would compact the open circular DNA. Surprisingly, IHF showed a much poorer affinity for the circular dimeric species I (right panel), suggesting that this species has a conformation unfavorable to IHF binding. The small amount of retarded complex observed is likely due to an increased molecular weight of the complex resulting from nonspecific association of IHF with this species.

To compare the relative stability of IHF bound to either the circular dimer II or the linear dimer, a gel retardation assay was carried out (Figure 11B). IHF was complexed with each of the two DNA species, challenged with a 40-fold excess of cold DNA for various times, and electrophoresed on native polyacrylamide gels. While IHF was 50% dissociated from the linear dimer in approximately 20 min, it remained completely bound to the circular DNA after 60 min. The data are graphically represented in Figure 11C. These results suggest IHF has a higher affinity for circular DNA than for linear DNA of the same length.

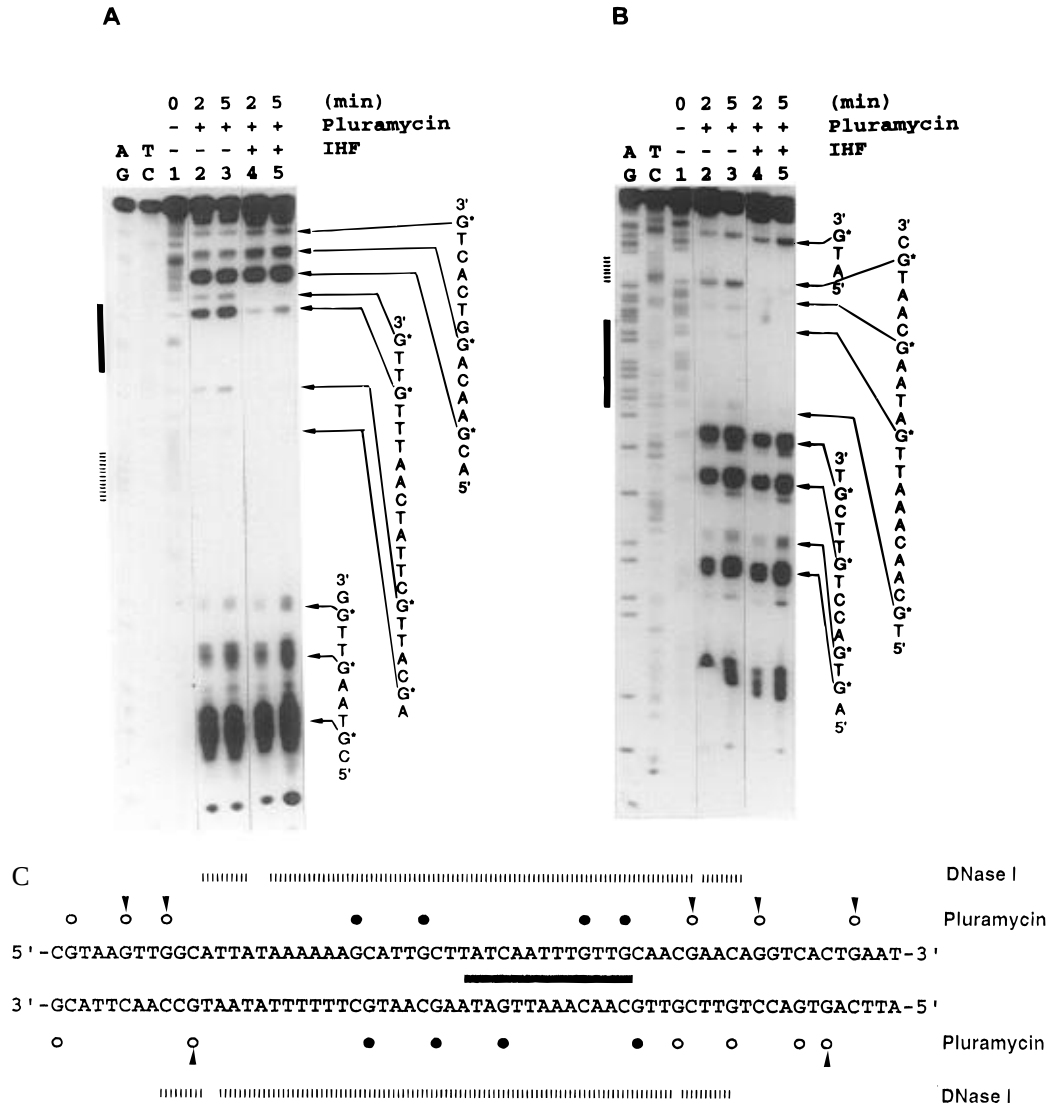

FIGURE 7: Time course of pluramycin modification of top (A) and bottom (B) strands of H′ DNA (oligomer I) in the absence (lanes 2−3) and presence of IHF (lanes 4−5). Lane 1, control DNA. Arrows indicate guanines modified with pluramycin. Reaction times with pluramycin are indicated. Other symbols are as in Figure 2. (C) Summary of pluramycin protection experiments. Closed and open circles indicate pluramycin protection and modification sites, respectively. Arrowheads indicate enhanced modification sites.

DISCUSSION

(+)-CC-1065 as a Probe for IHF-Induced DNA Bending. IHF is a sequence-specific DNA-binding protein proposed to recognize DNA primarily through the minor groove (Yang & Nash, 1989). Although unusual when first proposed, since discrimination between bases is poor in the minor groove (Seeman et al., 1976), such a mode of interaction is probable. For example, the cocrystal structure of the transcription factor TBP with its cognate site has now revealed an exclusively minor-groove interaction (Kim et al., 1993). In this study, we have used novel drugs to obtain more insight into the details of IHF−DNA recognition at the H′ site of phage λ. The results obtained are summarized in Figure 12.

Footprinting experiments with hydroxyl radicals, DMS, and DNase I were generally consistent with similar studies reported earlier for IHF−H′ DNA complexes (Yang & Nash, 1989). Our experiments revealed a more dramatic enhancement of hydroxyl-radical cleavages within the IHF interaction site (Figure 2), possibly because IHF−DNA complexes were gel-isolated after hydroxyl-radical treatment prior to analysis for strand breakage. The rate of cleavage of a particular nucleotide by hydroxyl radicals might conceivably be sensitive to the conformation of the deoxyribose as well as to the extent of protein−DNA contacts in the minor groove. DNA bends into the minor groove are proposed to bury the sugar hydrogens that are attacked by hydroxyl radicals, resulting in diminished cleavage by the short-lived hydroxyl radical. The presence of two prominent enhancements in the hydroxyl-radical cleavage pattern within the IHF contact region strongly suggests the presence of distortions of the DNA backbone between the three protected regions (Yang & Nash, 1989), consistent with severe DNA bending known to be induced within this region (Thompson & Landy, 1988).

The other feature shown in Figure 2 is the significant reduction in hydroxyl-radical cleavage within the sequence immediately flanking the consensus IHF recognition site. It is possible that some of these effects are due to the DNA bending induced by IHF, rather than direct protein contact, since alkylation of adenines in these regions does not show strong interference effects (Yang & Nash, 1989), in contrast to the adenines within the consensus sequence region. The results reported in this study are consistent with this possibility.

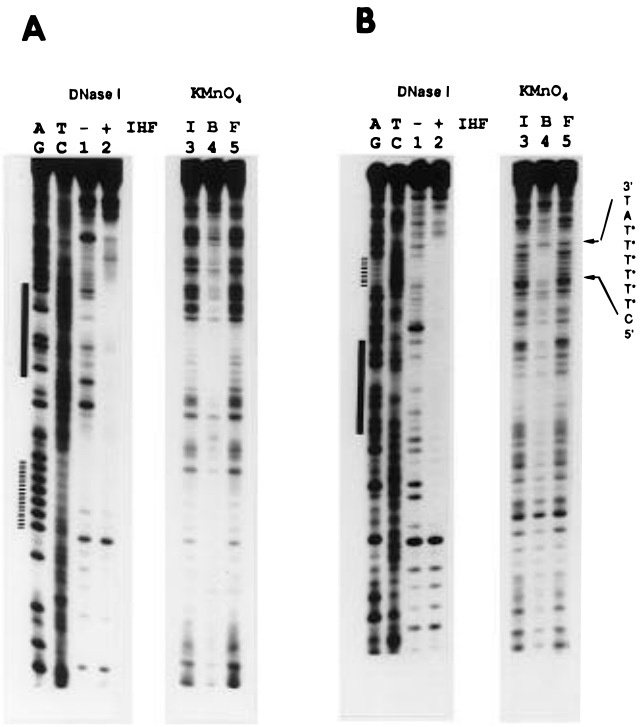

FIGURE 8: $KMnO_4$ protection of IHF−DNA complexes. Complexes were made with oligomer II and treated with $KMnO_4$, and IHF-bound and free forms of DNA were separated on a native polyacrylamide gel. They were subsequently isolated, cleaved with piperidine, and electrophoresed on denaturing polyacrylamide gels. (A) and (B) show the data for the top and bottom strands, respectively. Lanes 1 and 2 are DNase I cleavage patterns in the absence and presence of IHF. Lane 3 is control DNA treated with $KMnO_4$ in the absence of IHF. Lanes 4 and 5 are $KMnO_4$-treated DNA isolated from protein-bound and free DNA, respectively. All other symbols are as in Figure 3.

Because of the well-characterized and unique structure of a (+)-CC-1065-entrapped/induced bend in DNA and its structural similarity to A-tract bending, we have used (+)-CC-1065 in this study as a probe for monitoring IHF-induced DNA bending. Such bending could involve A-tracts or other sequences that may bend into the minor groove. Indeed, (+)-CC-1065 can still modify certain adenines within the upstream A-tract element in the presence of IHF, shifting the modification sites to the 5′-end relative to sites modified in free DNA, as seen in Figures 3−5. These modification sites lie within the region protected from DNase I and hydroxyl radicals by IHF, suggesting that changes in DNA structure induced by IHF, such as DNA bending in toward the minor groove, rather than direct protein contact, might be responsible for the reduction in magnitude of DNase I and hydroxyl-radical cleavage in this region. Furthermore, the presence of (+)-CC-1065 at these sites stabilizes the IHF−DNA complex (Figure 6), supporting the possibility that the bend induced by IHF binding to this sequence is recognized by (+)-CC-1065 as a favorable reactive site. As summarized in Figure 2C, DMS protection experiments have also revealed that the 3′-end of A-tracts at the 5′ upstream region is occupied by IHF through the minor groove (Yang & Nash, 1989). The demonstration of IHF−DNA cross-links with 3′ adenines in the A-tract (Yang & Nash, 1994), along with the results in this study, strongly support the idea that IHF makes contacts with the 3′-end of the A-tract upstream of the IHF core consensus sequence and induces DNA bending into the minor groove in its vicinity.

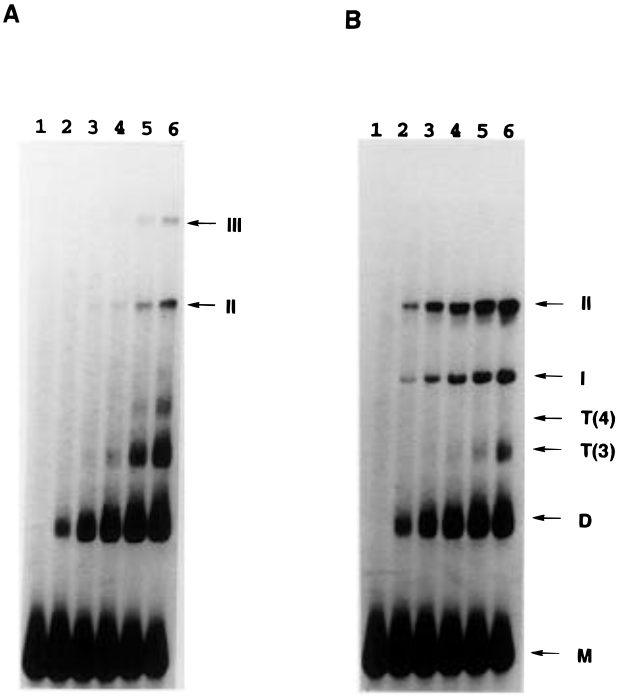

FIGURE 9: Influence of IHF on the distribution of T4 DNA ligase products. Ligation reactions in the absence (A) and presence (B) of IHF were carried out for various times using oligomer II as the substrate, as described in Experimental Procedures. Bands M, D, T(3), and T(4) correspond to linear monomer, dimer, trimer, and tetramer products, respectively. Bands I, II, and III are circular forms of the oligomer (see Figure 10 and text).

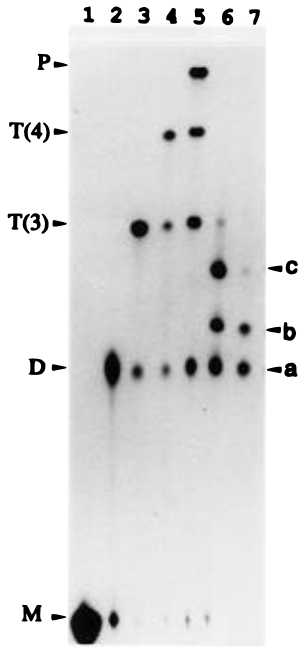

FIGURE 10: Characterization of DNA ligation products of IHF−DNA complexes. Products of ligation in the absence and presence of IHF (see Figure 9) were excised and electrophoresed on a 4% denaturing polyacrylamide gel. Lanes 1−5 contain linear multimers (from monomer to pentamer) produced in the absence of IHF, and lanes 6−7 contain DNA excised from bands I and II, respectively, from the ligation products obtained in the presence of IHF. a migrates at the position of a single-stranded linear dimer, while b and c migrate at positions likely for single-stranded and undenatured circular dimers, respectively (Ulanovsky et al., 1986).

As demonstrated during studies on the Mu transposase−DNA interaction, (+)-CC-1065 is a useful tool for discriminating protein protection sites from minor groove narrowing

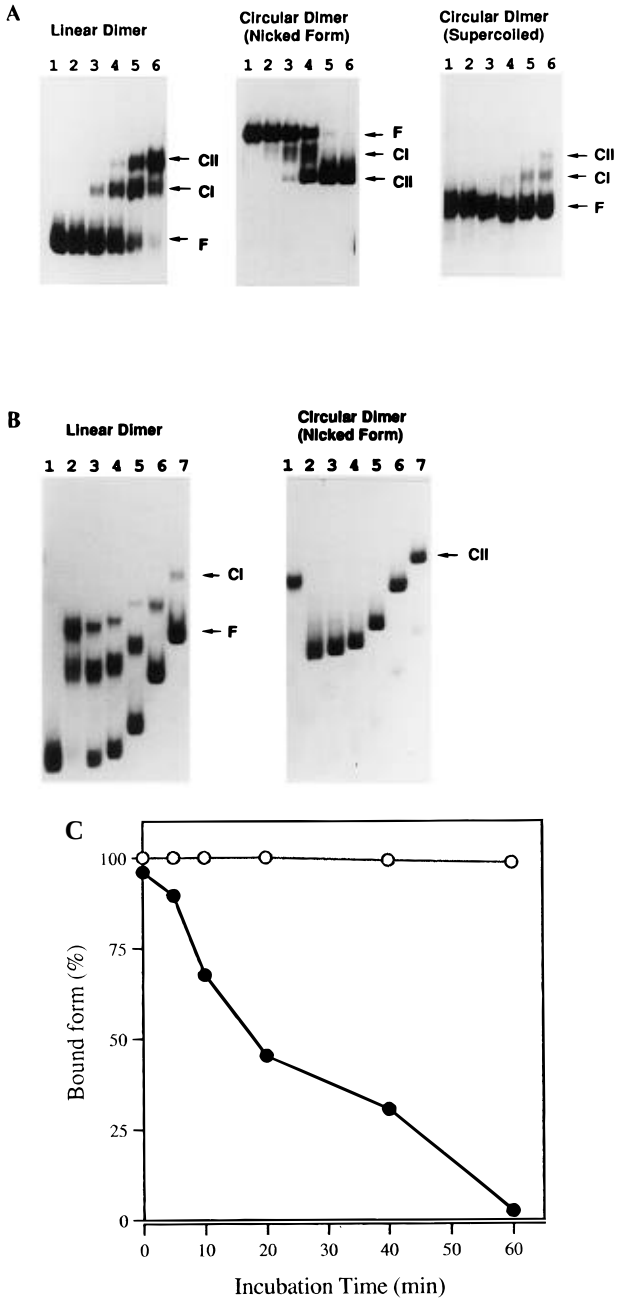

FIGURE 11: Measurement of IHF affinity for linear and circular dimeric DNA. (A) About 0.5 ng of each species of DNA substrate was incubated with 0, 0.05, 0.2, 0.5, and 1.0 ng of IHF (lanes 1−6), and the resulting complexes were analyzed by electrophoresis on a 5% native polyacrylamide gel. F, CI, and CII refer to DNA that is unbound or complexed with one or both sites in the dimer, respectively. (B) Measurement of the relative rates of dissociation of IHF from complexes with linear dimer and circular dimer II. IHF complexes formed with each of these species were challenged with a 40-fold excess of cold DNA for 0, 5, 10, 20, 40, and 60 min (lanes 2−7). Lane 1 contains DNA without IHF. (C) Graphical representation of data from (B). Open and closed circles represent the dissociation of IHF from the circular dimeric DNA and from the combined total of species CI and CII shown in panel B, respectively.

or bending sites (Ding et al., 1993). Our observation that (+)-CC-1065 is excluded from all its reactive sites within the IHF interaction region upon IHF binding (Figure 4) is consistent with the notion that the observed hydroxyl protection sites within this region are due to direct IHF−DNA contacts rather than indirect minor-groove bending induced from IHF interactions elsewhere.

Pluramycin and $KMnO_4$ as Probes for IHF-Induced DNA Unwinding and Base Unpairing. Structural and biochemical studies indicate that pluramycin intercalation into DNA and its alkylation of N7 of guanine are accompanied by DNA unwinding. Therefore, local unwinding of DNA is expected to facilitate pluramycin intercalation at these sites. We cannot, however, rule out that some other perturbation in DNA structure might facilitate pluramycin intercalation. Our results show that the pluramycin sites within the IHF consensus sequence on both DNA strands are protected from alkylation in the presence of IHF (Figure 7). Some of the protected guanines, which are located between the AT-rich region and the core consensus sequence, are not protected from methylation by DMS (see Figure 2C). Since pluramycin threads through and projects into both the minor- and major-groove sides of its intercalation site, while DMS exerts its effect on guanines solely on the major-groove side of DNA, this result strongly supports the notion that IHF recognizes its consensus sequence primarily through contacts within the minor groove. Since pluramycin can still react with guanines located in the region flanking the 5′- and 3′-sides of the consensus sequence, where IHF does not protect the DNA from DMS or hydroxyl radicals but does protect it from DNase I cleavage (Figure 12), there is likely no direct protein contact outside the region spanning the AT-rich element and the core consensus sequence. Moreover, pluramycin modification is specifically enriched at several guanines in the flanking regions in IHF-bound DNA. These results suggest that IHF binding to the consensus sequence not only generates possible unwound sites at the 5′- and 3′-sides, which might be kinetically accessible sites for pluramycin, but also that pluramycin modification of these sites stabilizes the IHF−DNA complex. Of interest is the enhanced pluramycin reactivity of DNA outside the large DNase I protected region (see Figure 7C), indicative of long-range effects of site-specific binding of IHF to DNA. These observations may be of functional significance in the many cellular roles ascribed to IHF [see Friedman (1988), Freundlich et al. (1992), and Goosen and van de Putte (1995)]. In particular, unwinding of regions close to promoters (where many IHF sites are located) may facilitate conversion of an initially closed RNA polymerase complex to an open one.

Reactivity of $KMnO_4$ toward bases can be improved by strand separation and diminished by formation of stable bent structures (Borowiec & Hurwitz, 1988; McCarthy et al., 1993). The absence of $KMnO_4$ reactivity with A-tract thymines might be due to the strong stacking interactions of A-tract thymines with one another (Hagerman, 1990; McCarthy et al., 1990). Our results show that $KMnO_4$ mainly protects the 3′-end of the A-tract thymines at the upstream AT-rich region. In addition, $KMnO_4$ reactivity toward the core consensus sequence was significantly diminished. All these results strongly suggest that IHF binding to the consensus sequence does not cause strand separation but does stabilize the bent structure formed within the upstream A-tract site. Lack of $KMnO_4$ sensitivity has also been observed upon IHF binding to the L1 site in the pL promoter of phage λ (Giladi et al., 1992).

DNA Bending As Revealed by DNA Cyclization Studies. IHF-induced DNA bending at the H′ site was studied by monitoring the products of T4 DNA ligase-mediated cyclization of short DNA fragments carrying this site. In the absence of IHF, dimeric and trimeric circular species are

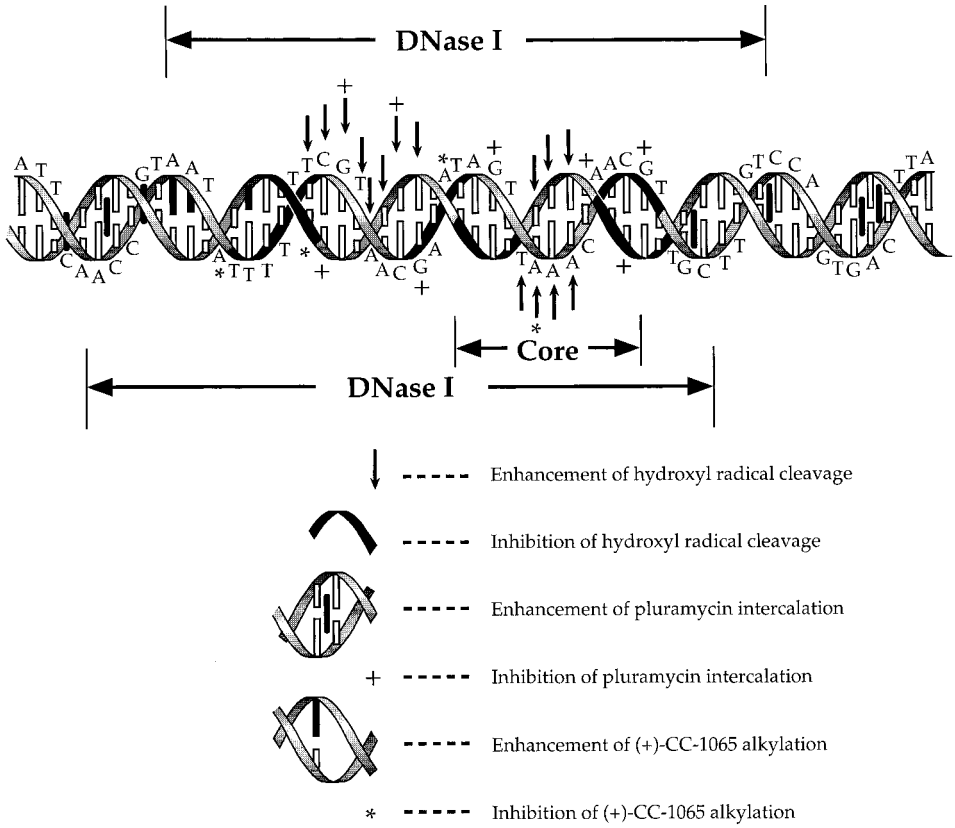

FIGURE 12: Summary of chemical and nuclease protection experiments of IHF−DNA complexes.

formed, while in the presence of IHF, the products of ring closure are exclusively dimeric (154 bp) (Figure 9). The complete absence of trimeric circles in the presence of IHF leads to an estimated overall IHF-induced bending angle close to 180°. This estimate is consistent with the results of Thompson and Landy (1988), who estimated a bend >140° at this site using a gel electrophoresis assay. Introduction of A-tracts designed to alter the direction of DNA curvature on either side of the IHF binding site had little effect on formation of the dimeric circles (unpublished results), suggesting that the large central bend induced by IHF overwhelms the additional A-tract bends.

Two well-resolved dimeric circular products were observed in the cyclization experiments (Figures 9 and 10). On native polyacrylamide gels, one of the circular species (I) had a faster mobility than the other (II), and its behavior in denaturing polyacrylamide gels as well as two-dimensional chloroquine gels was consistent with its being negatively supercoiled. Negative supercoiling could be introduced by IHF as a result of introduction of a DNA node upon either DNA bending or DNA unwinding. In support of this deduction, species I could be converted (albeit inefficiently) to II by the action of topoisomerase I. The poor reactivity with topoisomerase I could conceivably be a result of a DNA conformation of species I unfavorable to topoisomerase I binding, as evidenced by the inability of IHF to rebind this species (Figure 11A). Interestingly, species I always migrated as a single high-mobility band and could not be resolved into intermediate topological forms, even in the presence of high concentrations of counterions (unpublished data), conditions known to resolve topoisomers of supercoiled small circular DNA (Bednar et al., 1994). It is likely, therefore, that this species carries an additional DNA distortion [such as a kink (or kinks) associated with DNA bending] that would explain its behavior in the different experiments. As has been noted earlier (Yang & Nash, 1989), the enhanced hydroxyl-radical cleavage sites produced by IHF at the H′ site could represent widened minor grooves associated with the severe distortion of the DNA backbone that would be necessary to produce the sharp bend. We note in this context that TFIID, a minor-groove-specific protein related to IHF (Nash & Granston, 1991), has been shown to introduce two kinks in DNA, the region between the kinks being partially unwound with a widened minor groove (Kim et al., 1993). The inability of species I to rebind IHF (Figure 11A) may indicate that, due to the physical constraints associated with the small size of the circular species, the original distortion is altered or converted to a form (upon deproteinization) that prevents IHF from rebinding.

Gel-shift assays indicate that IHF binds more strongly to the dimeric circular species II (nicked form) compared to linear DNA (Figure 11A), suggesting that the bending associated with circularization of small DNA molecules (Kahn & Crothers, 1992; Pil et al., 1993) favors IHF binding. A similar observation has been made by Teter (1991). If a protein binds and bends DNA, it is likely that prebent DNA may present a more favorable conformation for protein interaction. It is known, for example, that although the various IHF binding sites all share the core consensus sequence, IHF differs markedly in its affinity for these sites [see Goosen and van de Putte (1995)]. The AT-rich element found upstream of the core consensus in the H′ site, for example, is not present at all IHF binding sites and is known to increase the affinity of IHF for DNA (Hales et al., 1994). Stabilization of this bend also increases the stability of IHF on the DNA, as seen in experiments using (+)-CC-1065 (Figure 6). The higher binding affinity of IHF for the small circular molecules compared to linear ones (Figure 11)

suggests that curved structures, such as those in preformed DNA loops, may be better *in vivo* targets for IHF. One such example is in the regulatory region of the osmolarity-sensing response of *E. coli*. High osmolarity results in a high degree of phosphorylation of OmpR, which binds to several upstream sites forming a repressive loop, blocking the expression of *ompF* (Slauch & Silhavy, 1991). IHF is thought to stabilize this DNA loop. In most known examples of IHF function, the DNA bend induced by IHF allows the juxtaposition and interaction of distantly located proteins [see Friedman (1988), Freundlich et al. (1992), and Goosen and van de Putte (1995)]. These newly created loops are likely to be stabilized in turn by the binding of IHF to the bent DNA. The short- and long-range DNA unwinding/distortion events induced by IHF are likely to play important roles in the biological function of IHF.

In summary, our results reveal that IHF interacts with the adenines on the 3′-side of the AT-rich element and likely induces a minor-groove bend in its vicinity. DNA modified at this site with (+)-CC-1065 stabilizes IHF interaction. DNA is likely unwound on the 3′-side of the core consensus sequence, as determined by increased intercalation of pluramycin. IHF-induced long-range effects on DNA were seen using this probe. Despite the structural distortions that produce increased hydroxyl-radical cleavage and increased pluramycin intercalation, no unpaired DNA segments were detected by $KMnO_4$ in the IHF interaction region. T4 ligase-catalyzed cyclization experiments have demonstrated a near-180° bend associated with IHF binding to the H′ site of phage λ. The properties of one of the circular species (I) are consistent with DNA strand crossing, unwinding, and distortion events associated with IHF binding. The stability of IHF on small open circular DNA is higher than that on linear DNA of the same length. These results may be relevant to the varied functions of IHF *in vivo*.

ACKNOWLEDGMENT

We are grateful to Howard A. Nash (NIH) for providing IHF protein, Howard Nash and Steve Goodman for comments on the initial version of the manuscript, and David Bishop for editorial assistance and preparation of the manuscript.

REFERENCES

Akman, S. A., Doroshow, J. H., & Dizdaroglu, M. (1990) *Arch. Biochem. Biophys. 282*, 202−205.
Bednar, J., Furrer, P., Stasiak, A., Dubochet, J., Egelman, E. H., & Bates, A. D. (1994) *J. Mol. Biol. 235*, 825−847.
Borowiec, J. A., & Hurwitz, J. (1988) *EMBO J. 7*, 3149−3158.
Burkhoff, A. M., & Tullius, T. D. (1987) *Cell 48*, 935−943.
Burkhoff, A. M., & Tullius, T. D. (1988) *Nature 331*, 455−457.
Ding, Z.-M., Harshey, R. M., & Hurley, L. H. (1993) *Nucleic Acids Res. 21*, 4281−4287.
Frantz, B., & O'Halloran, T. V. (1990) *Biochemistry 29*, 4747−4751.
Freundlich, M., Ramani, N., Mathew, E., Sirko, A., & Tsui, P. (1992) *Mol. Microbiol. 6*, 2557−2563.
Friedman, D. I. (1988) *Cell 55*, 545−554.
Giladi, H., Igarashi, K., Ishihama, A., & Oppenheim, A. B. (1992) *J. Mol. Biol. 227*, 985−990.
Goodman, S. D., Nicholson, S. C., & Nash, H. A. (1992) *Proc. Natl. Acad. Sci. U.S.A. 89*, 11910−11914.
Goodrich, J. A., Schwartz, M. L., & McClure, W. R. (1990) *Nucleic Acids Res. 18*, 4993−5000.
Goosen, N., & van de Putte, P. (1995) *Mol. Microbiol. 16*, 1−7.
Hagerman, P. J. (1990) *Annu. Rev. Biochem. 59*, 755−781.
Hales, L. M., Gumport, R. I., & Gardner, J. F. (1994) *J. Bacteriol. 176*, 2999−3006.
Hansen, M., Yung, S., & Hurley, L. H. (1995) *Chem. Biol. 2*, 229−240.
Hayatsu, H., & Ukita, T. (1967) *Biochem. Biophys. Res. Commun. 29*, 556−561.
Hurley, L. H., Reynolds, V. L., Swenson, D. H., & Scahill, T. (1984) *Science 226*, 843−844.
Hurley, L. H., Lee, C.-S., McGovren, J. P., Mitchell, M., Warpehoski, M. A., Kelly, R. C., & Aristoff, P. A. (1988) *Biochemistry 27*, 3886−3892.
Kahn, J. D., & Crothers, D. M. (1992) *Proc. Natl. Acad. Sci. U.S.A. 89*, 6343−6347.
Kim, J. L., Nikolov, D. B., & Burley, S. K. (1993) *Nature 365*, 520−527.
Kosturko, L. D., Daub, E., & Murialdo, H. (1989) *Nucleic Acids. Res. 17*, 317−334.
Lee, C.-S., Sun, D., Kizu, R., & Hurley, L. H. (1991) *Chem. Res. Toxicol. 4*, 21−26.
Lyubchenko, Y., Shlyakhtenko, L., Chernov, B., & Harrington, R. E. (1991) *Proc. Natl. Acad. Sci. U.S.A. 88*, 5331−5334.
McCarthy, J. G., Williams, L. D., & Rich, A. (1990) *Biochemistry 29*, 6071−6081.
McCarthy, J. G., Frederick, C. A., & Nicolas, A. (1993) *Nucleic Acids Res. 21*, 3309−3317.
Nash, H. A., & Granston, A. E. (1991) *Cell 67*, 1037−1038.
Panigrahi, G. B., & Walker, I. G. (1991) *Biochemistry 30*, 9761−9767.
Pil, P. M., Chow, C. S., & Lippard, S. J. (1993) *Proc. Natl. Acad. Sci. U.S.A. 90*, 9465−9469.
Reynolds, V. L., Molineux, I. J., Kaplan, D., Swenson, D. H., & Hurley, L. H. (1985) *Biochemistry 24*, 6228−6237.
Robertson, C. A., & Nash, H. A. (1988) *J. Biol. Chem. 263*, 3554−3557.
Sasse-Dwight, S., & Gralla, J. D. (1988) *Proc. Natl. Acad. Sci. U.S.A. 85*, 8934−8938.
Scahill, T. A., Jensen, R. M., Swenson, D. H., Hatzenbuhler, N. T., Petzold, G. L., Wierenga, W., & Brahme, N. D. (1990) *Biochemistry 29*, 2852−2860.
Seeman, N. C., Rosenberg, J. M., & Rich, A. (1976) *Proc. Natl. Acad. Sci. U.S.A. 73*, 804−808.
Slauch, J. M., & Silhavy, T. J. (1991) *J. Bacteriol. 173*, 4039−4048.
Sun, D., & Hurley, L. H. (1992) *Anti-Cancer Drug Des. 7*, 15−36.
Sun, D., & Hurley, L. H. (1994a) *Biochemistry 33*, 9578−9587.
Sun, D., & Hurley, L. H. (1994b) *Gene 149*, 165−172.
Sun, D., & Hurley, L. H. (1995) *Chem. Biol. 2*, 457−469.
Sun, D., Lin, C. H., & Hurley, L. H. (1993a) *Biochemistry 32*, 4487−4495.
Sun, D., Hansen, M., Clement, J. J., & Hurley, L. H. (1993b) *Biochemistry 32*, 8068−8074.
Sun, D., Hansen, M., & Hurley, L. H. (1995) *J. Am. Chem. Soc. 117*, 2430−2440.
Tanaka, I., Appelt, K., Dijk, J., White, S. W., & Wilson, K. S. (1984) *Nature 310*, 376−381.
Teter, B. (1991) Ph.D. Thesis, University of Southern California.
Thompson, T. F., & Landy, A. (1988) *Nucleic Acids Res. 16*, 9687−9705.
Ulanovsky, L., Bodner, M., Trifonov, E. N., & Choder, M. (1986) *Proc. Natl. Acad. Sci. U.S.A. 83*, 862−866.
Wang, S., Cosstick, R., Gardner, J. F., & Gumport, R. I. (1995) *Biochemistry 34*, 13082−13090.
Warpehoski, M. A., & Hurley, L. H. (1988) *Chem. Res. Toxicol. 1*, 315−333.
White, S. W., Appelt, K., Wilson, K. S., & Tanaka, I. (1989) *Proteins: Struct., Funct., Genet. 5*, 281−288.
Winkelman, J. W., & Hatfield, G. W. (1990) *J. Biol. Chem. 265*, 10055−10060.
Yang, C.-C., & Nash, H. A. (1989) *Cell 57*, 869−880.
Yang, S.-W., & Nash, H. A. (1994) *Proc. Natl. Acad. Sci. U. S. A. 91*, 12183−12187.

BI952786X